



This is a repository copy of *A practical green infrastructure intervention to mitigate air pollution in a UK school playground.*

White Rose Research Online URL for this paper:

<https://eprints.whiterose.ac.uk/196142/>

Version: Published Version

Article:

Redondo Bermúdez, M.D.C., Chakraborty, R. orcid.org/0000-0002-1063-2330, Cameron, R.W. et al. (2 more authors) (2023) A practical green infrastructure intervention to mitigate air pollution in a UK school playground. *Sustainability*, 15 (2). 1075. ISSN 2071-1050

<https://doi.org/10.3390/su15021075>

Reuse

This article is distributed under the terms of the Creative Commons Attribution (CC BY) licence. This licence allows you to distribute, remix, tweak, and build upon the work, even commercially, as long as you credit the authors for the original work. More information and the full terms of the licence here:

<https://creativecommons.org/licenses/>

Takedown



If you consider content in White Rose Research Online to be in breach of UK law, please notify us by emailing eprints@whiterose.ac.uk including the URL of the record and the reason for the withdrawal request.



eprints@whiterose.ac.uk
<https://eprints.whiterose.ac.uk/>

Article

A Practical Green Infrastructure Intervention to Mitigate Air Pollution in a UK School Playground

María del Carmen Redondo Bermúdez ^{1,*}, Rohit Chakraborty ² , Ross W. Cameron ¹, Beverley J. Inkson ³ and Maria Val Martin ^{4,*} 

¹ Department of Landscape Architecture, The University of Sheffield, Sheffield S10 2TN, UK

² Department of Civil and Structural Engineering, The University of Sheffield, Sheffield S1 3JD, UK

³ Department of Materials Science and Engineering, The University of Sheffield, Sheffield S1 3JD, UK

⁴ Plants, Photosynthesis and Soil, School of Biosciences, The University of Sheffield, Sheffield S10 2TN, UK

* Correspondence: maria.redondo@sheffield.ac.uk (M.d.C.R.B.); m.valmartin@sheffield.ac.uk (M.V.M.)

Abstract: Air pollution severely compromises children’s health and development, causing physical and mental implications. We have explored the use of site-specific green infrastructure (green barriers) in a school playground in Sheffield, UK, as an air-pollution-mitigation measure to improve children’s environment. The study assessed air quality pre-post intervention and compared it with two control sites. Nitrogen dioxide (NO₂) and particulate matter <2.5 μm in size (PM_{2.5}) concentration change was assessed via three methods: (1) continuous monitoring with fixed devices (de-seasonalised); (2) monthly monitoring with diffusion tubes (spatial analysis); (3) intermittent monitoring with a mobile device at children’s height (spatial analysis). De-seasonalised results indicate a reduction of 13% for NO₂ and of 2% for PM_{2.5} in the school playground after two years of plant establishment. Further reductions in NO₂ levels (25%) were observed during an exceptionally low mobility period (first COVID-19 lockdown); this is contrary to PM_{2.5} levels, which increased. Additionally, particles captured by a green barrier plant, *Hedera helix* ‘Woerner’, were observed and analysed using SEM/EDX techniques. Particle elemental analysis suggested natural and potential anthropogenic origins, potentially signalling vehicle traffic. Overall, green barriers are a valid complementary tool to improve school air quality, with quantifiable and significant air pollution changes even in our space-constrained site.

Keywords: air quality; air pollution; green infrastructure; green barrier; nature-based solutions; COVID-19 lockdown



Citation: Redondo Bermúdez, M.d.C.; Chakraborty, R.; Cameron, R.W.; Inkson, B.J.; Val Martin, M. A Practical Green Infrastructure Intervention to Mitigate Air Pollution in a UK School Playground. *Sustainability* **2023**, *15*, 1075. <https://doi.org/10.3390/su15021075>

Academic Editors: Vera Rodrigues and Sandra Rafael

Received: 8 December 2022

Revised: 24 December 2022

Accepted: 29 December 2022

Published: 6 January 2023



Copyright: © 2023 by the authors. Licensee MDPI, Basel, Switzerland. This article is an open access article distributed under the terms and conditions of the Creative Commons Attribution (CC BY) license (<https://creativecommons.org/licenses/by/4.0/>).

1. Introduction

Air pollution continues to be one of the most pressing challenges of the urban landscape, causing environmental quality decline and human health implications. In particular, children’s exposure to air pollution has severe repercussions to their health. At the same time, a shocking 93% of children under 15 years old breathe polluted air worldwide [1]. These children might have experienced a range of illnesses, from adverse neurodevelopment [2,3] and mental health problems [4], to decreased respiratory and cardiovascular functions [5,6]. Whilst tackling the sources of pollution remains the most recommended way to cut down toxic emissions and protect children’s health [7,8], the current implemented measures worldwide do not seem sufficient for the urgency of solving a mostly anthropogenic problem [9]. In that sense, additional mitigation measures to protect vulnerable populations have been explored, including the use of green infrastructure (GI) to reduce air pollution at a local level.

Under the nature-based solutions umbrella, GI encompasses any type of natural and semi-natural areas managed to deliver ecosystem services [10]. In the urban landscape, this translates into street trees, parks, green roofs, green walls, hedges, green barriers or fences, among others. GI has the potential to reduce ambient air pollution via multiple

mechanisms: gases absorption such as nitrogen dioxide (NO₂), gases and particulate matter (PM) deflection and dispersion, and PM deposition on plants' structures [11]. Simultaneously, various factors affect GI's performance to improve air quality (AQ), such as the urban layout and the local wind direction [12], or the plants' composition and their AQ functional traits [13,14].

The use of GI in school facilities to reduce pupils' exposure to air pollutants has been suggested by the U.S. Environmental Protection Agency [15]. Some schools have put the GI proposal into practice in the UK—specifically installing green barriers or fences. For instance, schools in Dorset and London have installed ivy panels around the school facilities' perimeter [16,17]; four schools in Manchester are part of a trial run by Lancaster University where evergreen hedges were planted between school premises and passing traffic [18,19]; and the Mayor of London's Green Fund awarded a grant to twenty-nine primary schools to plant vegetation and boost air quality [20]. Although purposely implemented green barriers exist in these UK schools, there is little/weak scientific evidence on actual air pollution concentration changes due to the GI intervention, and that consider the site's conditions. For instance, Abhijith et al. [21] found a 44% decrease of PM concentrations immediately behind a green screen installed in a London school, but the authors' short monitoring campaign did not take into account the effect of the site's seasonal and weather conditions, and COVID restrictions. Moreover, most research to date comprises AQ assessments in places with pre-existing GI onsite, which do not offer understanding of air pollution pre-post intervention or are based on modelling studies that present ideal situations for air quality improvement [13,22–28], potentially different from what could be achieved in intricate real-life school environments. Besides, most studies use simplistic GI formed by one to three plant species, e.g., [29], instead of more complex planting designs. GI composed of multiple species could foster ecosystem functioning and deliver co-benefits (e.g., safety, wellbeing, aesthetics, biodiversity).

This study assesses AQ impacts of a multi-species (31 taxa) thin GI in a UK school playground, where a green barrier was purposely built and designed as a functioning ecosystem that fits the irregular school layout. Pre- and post-intervention conditions—including air quality, meteorological conditions, and COVID restrictions—are fully acknowledged and characterised. Here, we focus on evaluating the GI intervention in terms of NO₂ and PM_{2.5} concentration changes, and on identifying the composition of the latter. The following sections elaborate on the methods (Section 2), the AQ outcomes due to the green barrier implementation and a discussion based on three research questions (Section 3):

- (i) Can site-specific multi-species thin green barriers provide enough protection against NO₂ and PM_{2.5} air pollution in a school facility?
- (ii) What is ambient PM around an inner-city school made of?
- (iii) What has a larger influence on school air quality: multi-species thin green barrier implementation or low-vehicle traffic (due to COVID-19 lockdown)?

Concluding remarks are presented in Section 4.

2. Materials and Methods

2.1. Study Design

A green barrier was installed in a case study school in Sheffield, UK. Air quality was monitored pre and post such GI intervention at the case study school (Sch-GB site) and at two other sites serving as control for data comparison and contrast (Figure 1). The control sites are located within a 2 km radius from Sch-GB and comprise a site in the city centre (City site)—providing an urban background—and another school playground without a green barrier (Sch-NoGB site). Air quality was monitored at those three sites from April 2019 to October 2021 (Figure 2). Sources of air pollution at the study sites include motorised transport and residential/commercial forms of burning, such as woodburning stoves. In Sheffield, 81% of road transport accounts for cars and taxis, while the remaining 19% includes buses, light vans, heavy goods vehicles, and motorcycles [30].

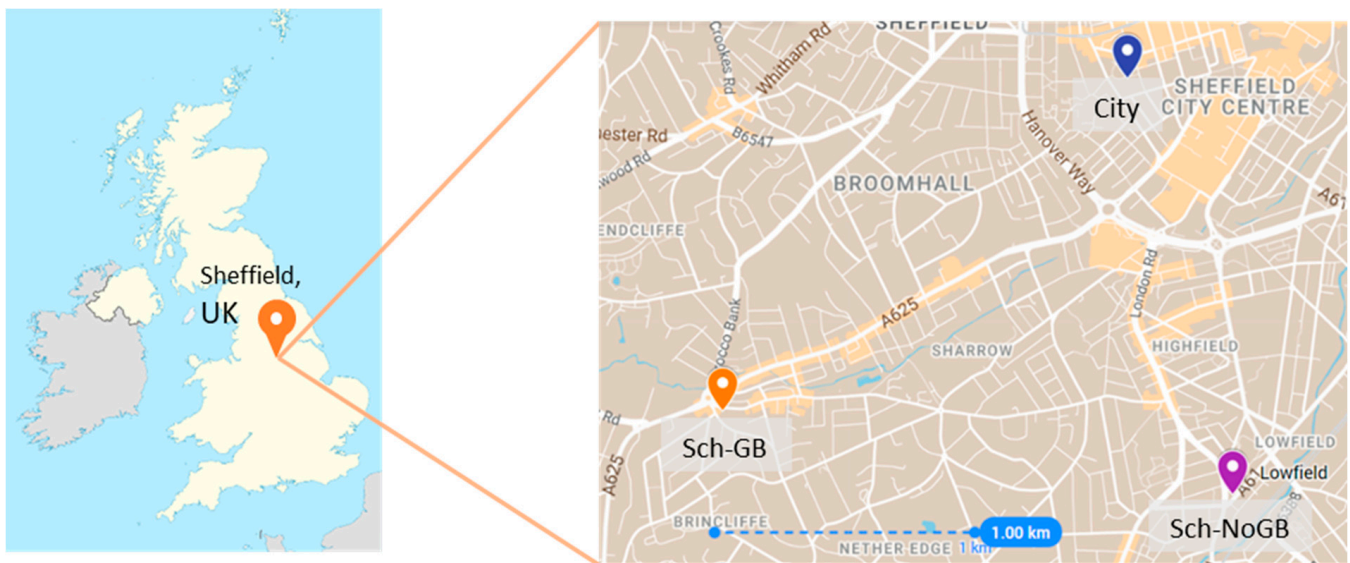


Figure 1. Location of the study sites for air quality monitoring in Sheffield, UK. ‘Sch-GB’ refers to case study school with a green barrier; ‘City’ refers to a city centre site (control); ‘Sch-NoGB’ refers to an urban school site without a green barrier (control).

In light of the study happening during COVID-19 pandemic times, which caused citizen’s mobility and ‘normal’ activities disruptions due to UK governmental restrictions and lockdowns to contain the spread [31], only three periods from the AQ campaign were adequate for analysis and comparison (Table 1). These periods were most similar in vehicle traffic flow and comprised the same months for each year of the study. Vehicle traffic flow (vehicle h^{-1}) data are reported for each period and site in Table 2. These data were collected at a 1 h resolution from the Urban Flows Observatory portal [32], which compiled data recorded by Sheffield City Council. Additionally, a period of low-vehicle traffic and low-citizens’ mobility (first lockdown April–June 2020) was selected for contrast and comparison with the three other periods Table 1. Figure 2 shows the study’s timeline with the data-collection periods.

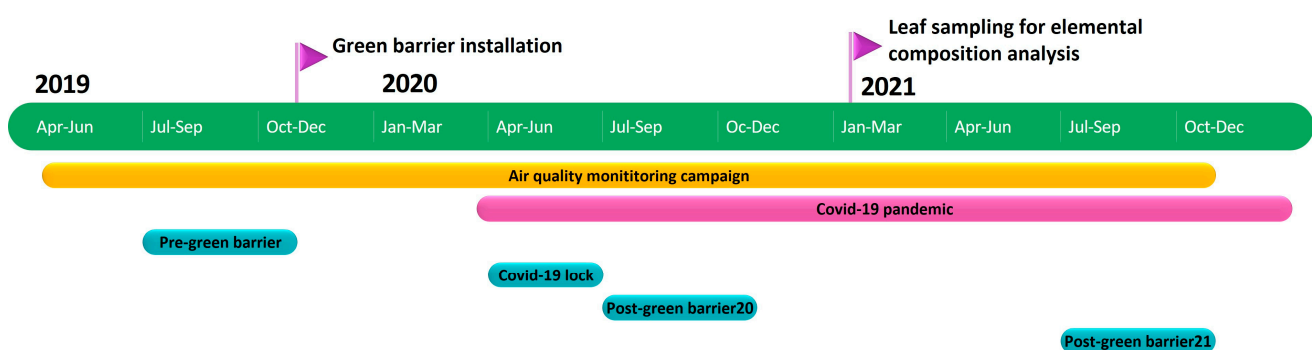


Figure 2. Air quality data-collection periods. Blue colour represents periods selected for data analysis.

Table 1. Periods selected for air quality assessment from the study’s data-collection campaign.

Data Collection Period	Abbreviation	Date	Description
Pre-green barrier	pre-gb	July–October 2019	Baseline period: before the green barrier was implemented in Sch-GB site’s playground.
COVID-19 lockdown	lock	April–June 2020	Period after the green barrier implementation with first national lockdown measures to contain the COVID-19 pandemic. Vehicle traffic and citizens’ mobility were highly restricted.
Post-green barrier20	post-gb20	July–October 2020	Period one year after the green barrier implementation. COVID-19 restrictions were eased from 23 June to 31 October 2020. Second national lockdown came in force on 5th of November 2020.
Post-green barrier21	post-gb21	July–October 2021	Period two years after the green barrier implementation. Last phase of COVID-19 pandemic restrictions ease, and full reopening of all economic activities on 19 July 2021.

Table 2. Mean traffic flow (vehicle h⁻¹) at closest sensors to the study sites, per selected periods.

Period	Site		
	Sch-GB Mean ± SE	City Mean ± SE	Sch-NoGB Mean ± SE
pre-gb	331.2 ± 4.2	231 ± 3.6	NA
lock	197.4 ± 3.6	83.4 ± 1.8	268.2 ± 3.6
post-gb20	303.0 ± 4.2	160.2 ± 2.4	386.4 ± 3.6
post-gb21	342.0 ± 9.0	200.4 ± 3.0	463.2 ± 4.8

2.2. Green Infrastructure Intervention

A purposely designed multi-species green barrier—the GI intervention—was installed at the case study school (Sch-GB site). Such a green barrier was co-designed and co-produced with the school community and many other contributors participating in six project stages from October 2018 to January 2020 (so called GF-Sheff project). The project stages included introduction and goal setting, green barrier design, construction, planting, project debriefing, and maintenance [33].

The case study school has one- and two-story buildings of late-Victorian character, and an active and highly used playground that accommodates 270 pupils in the infant stage (5–7 years old) throughout the day. During pupils’ drop-off (8:50 h) and pick-up times (15:10 h), parents and children walk through the playground and socialise. From 10:30 h to 15:00 h, the playground is used on and off for play and lunch activities. Additionally, one day a week the playground is used for sports all-day-long, and extra-curricular sports club take place twice a week up to 16:15 h.

Before the green barrier was installed, the playground had only a low stone-wall (0.6–0.7 m high) and spaced metal railings (which allowed air flow) as a separation from the adjacent streets (Figure 3). These streets are in close proximity to the school, between 1.9–2.2 m away from the playground’s perimeter. Motorised vehicle traffic continuously circulates around the school, and car parking is available on one street adjacent to the playground (Figure 4). Moreover, residential and commercial facilities dominate the area. Therefore, local air pollution sources include vehicle traffic, and domestic and commercial activities.

The green barrier construction started in July 2019 with groundworks preparations and culminated in late October 2019 with local community’s supported planting (Figure 2).

The multi-species green barrier comprises a mix of 31 different taxa planted along the playground's border (Figure 4), which extends for 60 m. Its height ranges from 2.2 to 2.4 m; causing a separation between the playground and the street traffic of: 2.4 m max on the southwest portion of the playground, and 4.4 m max on the northwest corner and north portion of the playground (raised school grounds, Figure 4). Its width is 0.9 m continuously, except on the northwest corner of the playground, where it extends up to 1.3 m. Five taxa act as the green barrier's structural plants and are the key components of air pollution deposition, deflection, and dilution. The remaining taxa are complementary plants that support the ecosystem functioning of the planting scheme (fostering plant establishment, life-span extension, and a thriving planting scheme), add sensory interest, and create a more aesthetic design. All the plants were incorporated in an almost-mature stage that created a low-porosity green barrier, providing an immediate screening effect. Further information on the characteristics of the green barrier and the species used can be found in previous studies [33,34]. Pictures of the Sch-GB site before and after the green barrier implementation are depicted in Figure 3, and Figure 4 provides detailed information on the taxa used for the green barrier and its planting design in the school playground.

View from inside the playground

View from street

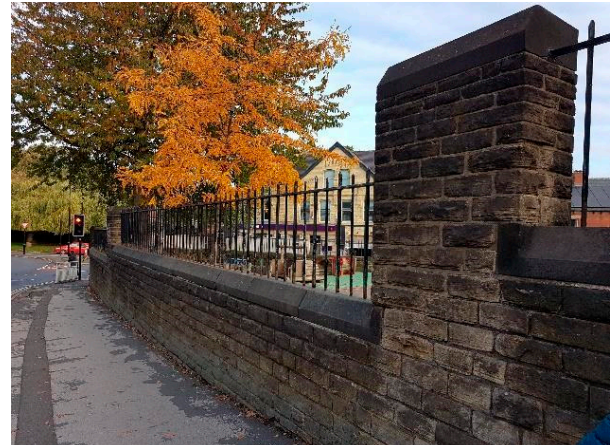
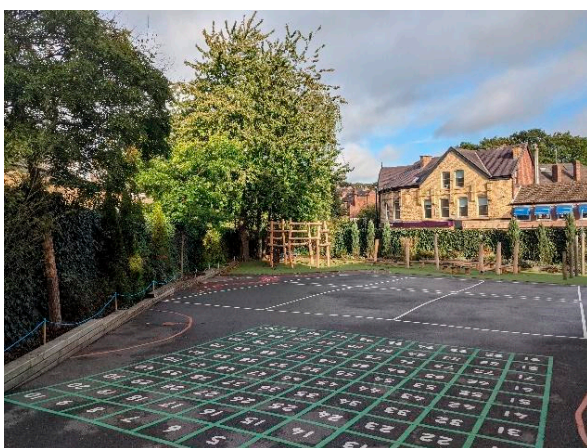
Before
green
barrier
imp.After
green
barrier
imp.

Figure 3. Pictures of the case study's school playground before and after the green barrier implementation (Sch-GB site).



Plant Name	Planting Plan Code	Plant Name	Planting Plan Code
Structural Plants		Herbaceous Plants	
<i>Hedera helix</i> 'Woerner'	Hed Woerner	<i>Alchemilla mollis</i>	Alc mol
<i>Juniperus scopulorum</i> 'Blue Arrow'	Jun Blu	<i>Anemanthele lessoniana</i>	Ane les
<i>Thuja occidentalis</i> 'Smaragd'	Thu SMA	<i>Asplenium scolopendrium</i>	Asp sco
<i>Chaemacyparis lawsonia</i> 'Ivonne'	Cha Ivo	<i>Bergenia cordifolia</i> 'Purpurea'	Ber Pur
<i>Phyllostachys nigra</i>	Phy nig	<i>Calamagrostis x acutiflora</i> 'Karl Foerster'	Cal KF
Shrubs		<i>Deschampsia caespitosa</i> 'Goldtau'	Des Gol
<i>Choisya ternate</i>	Cho ter	<i>Geranium endressii</i> 'Wargrave Pink'	Ger War
<i>Cornus alba</i> 'Sibirica'	Cor Sib	<i>Heuchera micrantha</i> 'Palace Purple'	Heu PP
<i>Cornus sanguinea</i> 'Midwinter Fire'	Cor MF	<i>Liriope muscari</i> 'Big Blue'	Lir Big
<i>Erica carnea</i> 'Springwood Pink'	Eri SP	<i>Nepeta</i> 'Six Hills Giant'	Nep SHG
<i>Erica carnea</i> 'Springwood White'	Eri SW	<i>Polystichum setiferum</i>	Pol set
<i>Euonymus fortuneii</i> 'Emerald Gaiety'	Euo Eme	<i>Salvia officinalis</i> 'Purpurescens'	Sal Pur
<i>Fatsia japonica</i>	Fat jap	<i>Sedum spectabile</i> 'Brilliant'	Sed Bri
<i>Hypericum</i> 'Hidcote'	Hyp Hid	<i>Stachys byzantina</i> 'Big Ears'	Sta Big
<i>Lavandula angustifolia</i> 'Hidcote'	Lav Hid	<i>Verbena bonariensis</i>	Ver bon
<i>Rosmarinus officinalis</i> 'Miss Jessopp's Upright'	Ros MJU	<i>Sarcococca confusa</i>	Sar con

Figure 4. Planting plan of the green barrier at the Sch-GB site. Blue arrows depict prevailing wind directions, size represents frequency. Modified from Urban Wilderness.

2.3. Air Quality Data Collection

To assess the air pollutants concentration change due to the installation of the green barrier, collection and assessment of AQ data was carried out at the three monitoring sites (Sch-GB as site with GI intervention; and City and Sch-NoGB as control sites), and during the different sampling periods (pre-gb, lock, post-gb20, postgf-21). Concentrations were measured for NO₂ and PM_{2.5} via three methods: (1) NO₂ and PM_{2.5} continuous monitoring with fixed devices at all monitoring sites, (2) NO₂ monthly monitoring with diffusion tubes at all monitoring sites, and (3) complementary spatially distributed PM_{2.5} monitoring with a mobile device in Sch-GB. AQ monitoring with fixed devices and diffusion tubes is fairly recognised by the scientific community and used by governments. In addition to these commonly used methods, we used a mobile device set up at children's breathing height (1.1 m) to understand spatial changes of air pollution in the place where children walk and play. Meteorological conditions were recorded using a weather station (OTT MetSystems) installed at Sch-GB. The weather station measured air temperature, relative humidity, air pressure, wind speed and direction, precipitation intensity, and global radiation in 15 min intervals. Details of each AQ data-collection method are described in the following sections.

2.3.1. Continuous Monitoring with Fixed Devices—NO₂ and PM_{2.5}

Each study site had a fixed AQ monitor measuring air pollutant concentrations continuously through the day. Therefore, NO₂ and PM_{2.5} data were extracted from each monitor's data portal at a 1 h resolution. Consequently, 24 measurements (in µg m⁻³) were collected per air pollutant for each day of the data-collection periods. Data were available for all sites and all periods, except for NO₂ during lock and post-gb20 periods at Sch-GB site.

The use of the selected fixed AQ monitors elaborates on previous AQ research conducted in Sheffield by Chakraborty et al. [35] and Munir et al. [36]. Details of each monitoring device corresponding to the study sites are shown in Table 3. City and Sch-NoGB sites have reference sensors managed by UK Department for Environment, Food and Rural Affairs (DEFRA), and Sheffield City Council, correspondingly. For the Sch-GB site, a low-cost monitor (AQ Mesh V5.0, Stratford upon Avon, UK) with medium accuracy was installed in the school facilities (Figure 5). This monitor's performance is reliable [37] and has been used in several studies [38–41], including school facilities [42,43]. It has an internal weather sensor that corrects data for weather effects using proprietary software, and data are also O₃-filtered to correct for cross-gas effects (eliminating O₃ sensitivities and providing accurate NO₂ concentrations). To refine data quality, concentrations from Sch-GB's monitor were scaled via a correlation with the reference sensors at the control sites.

2.3.2. Monthly Monitoring with Diffusion Tubes—NO₂

Diffusion tubes provided by Sheffield City Council were installed inside Sch-GB's playground in three different locations (Figure 5) to measure NO₂ concentrations. This AQ monitoring technique is part of the UK government tools utilised to review and assess mean annual NO₂ concentrations [47]. Diffusion tubes are passive samplers of atmospheric NO₂ and provide monthly indicative measurements. Atmospheric NO₂ reacts with the tubes' coated triethanolamine (TEA) cap and, after chemical analysis (colorimetry) by the correspondent laboratory, NO₂ monthly concentrations are calculated and provided [48].

Sheffield City Council manages a network of diffusion tubes in the city, which includes monitoring at Sch-NoGB and City study sites [49]. Therefore, Sch-GB NO₂ concentrations were compared within the playground and also with the control sites for the four data-collection periods (pre-gb, lock, post-gb20, and post-gb21). Local and national co-location studies of diffusion tubes with reference monitors take place every year to adjust NO₂ results. Bias adjustment is already reflected here and included correcting the data with bias adjustment factors from Sheffield City Council studies. These factors are 0.98, 0.93 and 0.93 for 2019, 2020 and 2021, correspondingly. It is worth noting that there are NO₂ measurements for each month of the data-collection periods, except for the lock period

at Sch-GB, which only has data from June 2020 due to COVID-19 disruptions; and the post-gb20 period at Sch-NoGB, which is missing data from July 2020.

Table 3. Fixed air quality monitors specifications for each study site.

Study Site	Air Quality Monitor Type	Air Quality Monitor Specifications	Monitoring Technique	Ref.
Sch-GB (green barrier intervention)	Low-cost (medium data accuracy) Data quality: <ul style="list-style-type: none"> Proprietary software for air pollutant concentration correction from cross-gas effect and from cross-interference with environmental conditions, developed by the manufacturer. Data correlation and scaling with reference sensors. 	AQ Mesh V5.0 Developed by Environmental Instruments Ltd. Monitor at 1.7 m above ground level, 3 m away from closest road	NO ₂ : Electrochemical PM _{2.5} : Optical particle counter	[36,37,44]
City (control site—city centre)	Reference (high data accuracy)	Monitoring station from DEFRA's AURN Station from ground level to 3 m high, 15 m away from closest road	NO ₂ : Chemiluminescence PM _{2.5} : Tapered Element Oscillating Microbalance	[36,45]
Sch-NoGB (control site—school)	Reference (high data accuracy)	Monitoring station from Sheffield City Council Station from ground level to 2.5 m high, 3.5 m away from closest road	NO ₂ : Chemiluminescence PM _{2.5} : Tapered Element Oscillating Microbalance	[36,46]

2.3.3. Intermittent Monitoring with a Mobile Device—PM_{2.5}

To complement the fixed AQ monitoring at Sch-GB and understand the spatial distribution of air pollution at children's breathing height (1.1 m), a low-cost mobile device (Aeroqual series 500) was used. It measured PM_{2.5} (via optical particle counter), temperature, and relative humidity at eight different locations. Five sampling locations are inside the school playground and three are located on the adjacent streets (Figure 5). Air sampling includes high-pollution times during the school day (pupil's drop-off and pick-up times), which were previously identified via the fixed-monitor data. Data collection took place from May–July and September–October 2019 (pre-gb), and from September–October 2020 (post-gb20). During the data-collection periods, PM_{2.5} and meteorological conditions (humidity and temperature) were collected with 1 min resolution at each sampling point, for 5 consecutive minutes at a time. A total of 2074 observations were collected and used for analysis. Due to the mismatch of pre and post green barrier collection periods, caused by COVID-19 disruptions, data were clustered by its meteorology. This meant that pre and post GI intervention data with the same mean humidity and temperature were compared. Data clusters included (1) high humidity (81%) and low temperature (14 °C) days, and (2) low humidity (52%) and high temperature (20 °C) days. These thresholds were selected to have similar number of observations pre-post intervention. The same mobile monitoring device (Aeroqual) has been successfully used in other studies [22,50–52]. Moreover, to improve data quality we conducted a field co-location with the MOBIUS (MOBIle Urban Sensing vehicle) reference sensor from the Urban Flows Observatory, The University of Sheffield [53] (Figure S2 in Supplementary Material).

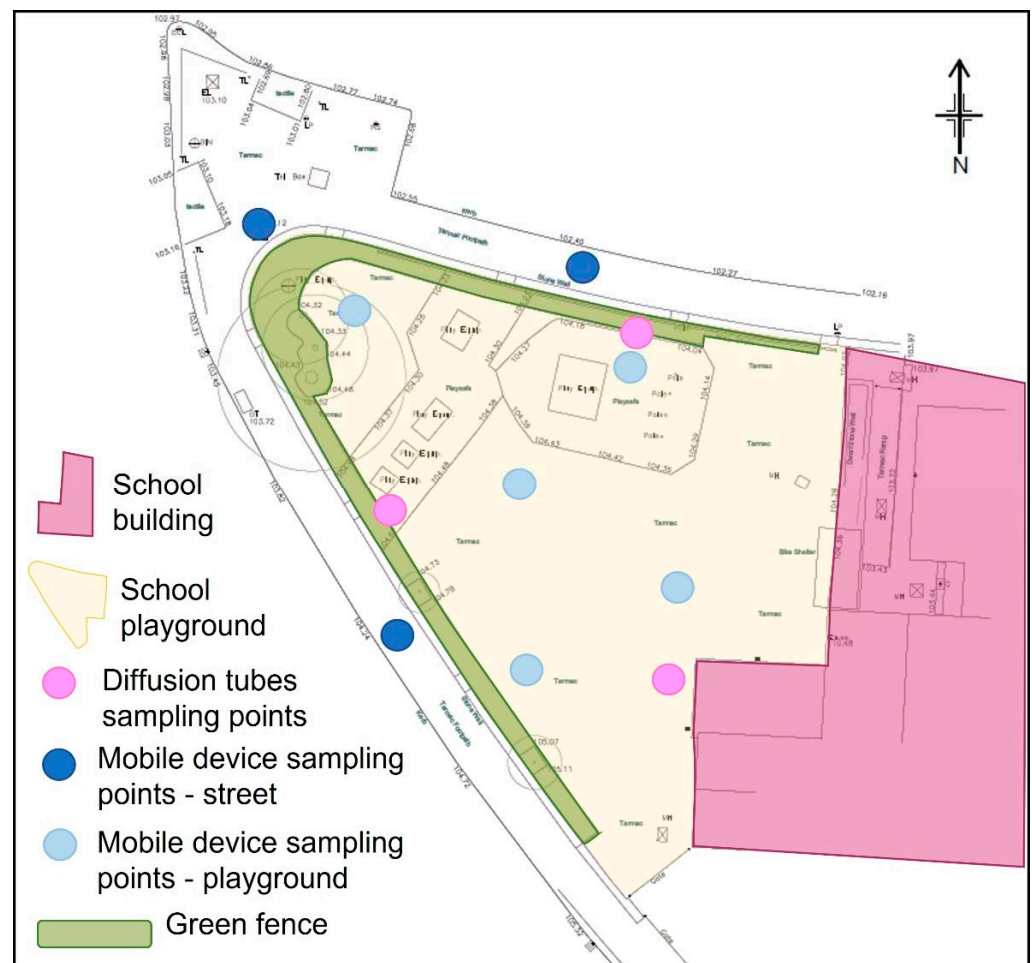


Figure 5. Air quality sampling locations in the case study school (Sch-GB) for diffusion tubes (NO_2), mobile low-cost device ($\text{PM}_{2.5}$), and fixed low-cost monitor (NO_2 and $\text{PM}_{2.5}$).

2.4. Air Quality Assessment

To assess the impact of the GI intervention on school air quality, we carried out a comparison of air pollutant concentration changes from the baseline period (pre-gb) to the three post green barrier periods (i.e., lockdown, post-gb20 and post-gb21) for Sch-GB within itself, and with the control sites. Air quality data were processed in a combination of Excel, R software, and Python programming languages, and general statistics were evaluated to calculate air pollutants concentration difference (in %), according to Equation (1):

$$[\text{NO}_2 \text{ or } \text{PM}_{2.5}] \text{ difference (\%)} = \left(\frac{[P_x] * 100}{[P_0]} \right) - 100 \quad (1)$$

where P_x represents either NO_2 or $\text{PM}_{2.5}$ mean concentrations at each study period (one at a time), and P_0 represents the mean concentration of the same air pollutant during the pre-gb period. Due to different baseline concentrations at each study site, air pollutant concentration differences (in %) were comparable across the city, unlike raw concentrations.

Prior this computation, fixed-monitor data were subjected to de-seasonalisation (Section 2.4.1) to reflect the sole effect of the green barrier more accurately. On the other hand, diffusion tubes and mobile device data maintained the influence of the weather; therefore, their results reflect it and were primarily used for qualitative spatial analysis (Section 2.4.2).

2.4.1. Data De-Seasonalisation

The global COVID-19 pandemic resulted in significant heterogeneity in recorded trends of anthropogenic emissions across the time under study. Variations in air quality as measured are also strongly impacted by meteorological conditions. As in previous studies that investigated the effect of COVID-19 restrictions on air quality [54–57], we eliminated these uncertainties using a de-seasonalising approach. After treating missing data and removing outliers, we used a two-step approach—using the R package ‘deweather’ [58]—to exclude the effect of trend and weather on the air quality data and to normalise them, as detailed below.

i. Step 1—Deweather:

We used the ‘gbm’ package to investigate and adjust for non-linear relationships between meteorological variables, air quality measurements, and temporal variables, to forecast the variability associated with the hour of the day, day of the week, and week of the year. The latter factored in seasonal weather factors that were not considered by the other components. Additionally, we included a trend term to account for COVID-19 related changes in emission patterns during the three-year study period via a Machine Learning (ML) technique based on the Generalized Boosted Regression Tree Model (BRT) [59]. The model is formed, as shown in Equation (2):

$$[PM_{2.5}] = RH + \bar{u} + trend + \emptyset + T\theta + t_{hour} + t_{weekday} + t_{JD} \quad (2)$$

where RH is relative humidity, \bar{u} is the mean hourly wind speed, $trend$ represents annual variations, \emptyset is the mean hourly wind direction (degrees, clockwise from the north), and $T\theta$ is the mean hourly temperature ($^{\circ}C$). Variables representing hour of the day, t_{hour} , day of the week, $t_{weekday}$, and day of the year, t_{JD} , were also considered for the model development.

For each site, 80% of the hourly meteorological and pollutant measurements were used for training the BRT model, with the remaining 20% split for testing and validation, with the goal of developing the most suitable model. This determination is achieved automatically using commonly used metrics such as Pearson’s correlation coefficient (r), root mean square error (RMSE) and mean bias (MB). Individual models were developed for $PM_{2.5}$ and NO_2 for the time of the study.

ii. Step 2—Meteorological normalisation:

We used the ‘metSim’ function to create meteorological simulations in order to validate the model and make predictions. After developing the model, the meteorological averaging process was used to predict weather conditions numerous times using random sampling [60]. The ‘metSim’ function was used to perform this sampling. The final model was developed to forecast concentrations while accounting for the change in trends caused by COVID-19 restrictions and meteorological variability. This method predicts concentrations that are representative of typical meteorology accounting for the covariates (temperature, humidity, wind speed, wind direction, week of the year, weekday, hour of the day, and trend). The model’s performance was evaluated using tenfold cross-validation. The model fitting results and the relation between $PM_{2.5}$, NO_2 , and the covariates are shown in Figure S1 (Supplementary Material).

2.4.2. Air Quality Pattern Trends

To characterise overall air quality trends of each study site, air pollutant concentrations were analysed using the ‘Theil-Sen’ tool built-in ‘Openair’ R package [61]. The approach provided a non-parametric measurement of trends based on ‘the median of the slopes of pairs of points with varied x-values’, slope estimation, and bootstrap uncertainty estimate [56]. Because these trends during lockdown vary from prior years and may obscure the results, leading to incorrect conclusions, they were removed using a process similar to weather normalisation. De-seasonalised modelled data (15 min resolution) filled the vacant periods and a trend between 2019 and 2020 was established. ‘Theil-Sen’ calculated

the monthly mean concentrations and the slopes between all pairs of the data. The final 'Theil-Sen' estimate of the slope (Figure 6) is the median of all these slopes. Air quality pattern trends aid to understand pollution over time at Sch-GB and the control sites, and to observe the green barrier's effect on AQ. Statistical significance to the p -value < 0.001 was determined from the trends' overlaid slope at the 95% confidence intervals.

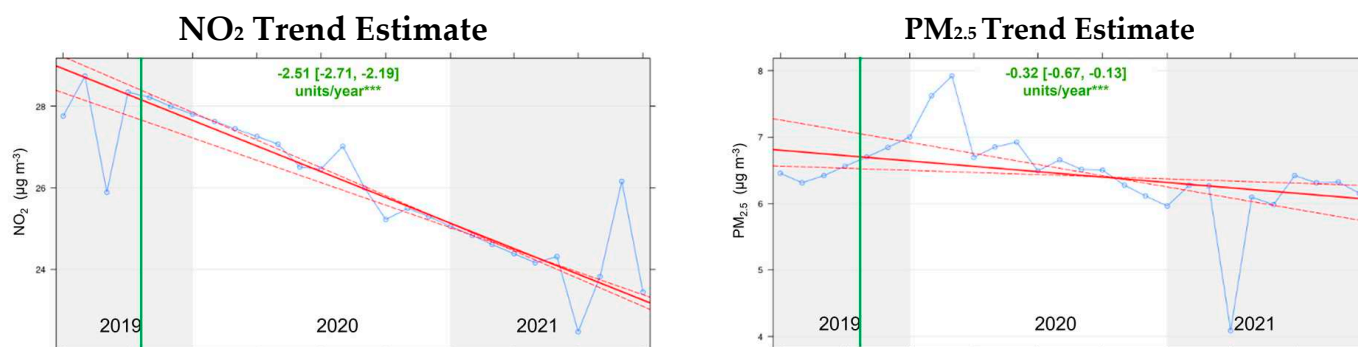


Figure 6. De-seasonalised mean NO_2 and $\text{PM}_{2.5}$ concentration trends (blue line, in $\mu\text{g m}^{-3}$) at Sch-GB site across time using de-seasonalised modelled data. The green vertical line represents the green barrier installation in the playground. The solid red line represents the overall trend estimate, and the dashed red lines represent 95% confidence intervals for the trend based on resampling methods. *** Shows that the trend is statistically significant at $p < 0.001$.

2.4.3. Qualitative Spatial Analysis

Diffusion tubes (NO_2) and mobile low-cost device ($\text{PM}_{2.5}$) data were primarily used for spatial analysis. Their timeframe, combined with the ease of monitoring across space, make them more suitable for qualitative analysis in geographical visualisations. Therefore, data were mapped at playground and city scale. This analysis provides a valuable visualisation tool to extract detailed information on pollutants concentration change across the playground and city.

2.5. Qualitative PM Elemental Composition Identification

A green barriers' mechanism of action to reduce air pollution is PM deposition on the plants' surface. In order to identify the sources of ambient PM in the case study school, we carried out an elemental composition analysis of the particles deposited on the leaves' surface of *Hedera helix* 'Woerner', the plants that cover the full length of the green barrier (Figure 4). Six leaf samples were collected in January 2021 at 1.25 m height from the school ground (Figure 2). They were stored in plastic containers, attaching the stem to the bottom of the container to prevent movement during transportation. The samples were observed under a scanning electron microscope (SEM) (Tescan Vega3 LMU) to visually examine and chemically analyse the particles deposited on the surface [34]. The SEM was used at 15 kV, in low vacuum mode (LVM) with a low vacuum secondary electron detector (LVSED). No conductive coating was applied to the leaves. Energy dispersive X-ray analysis (EDX) (Oxford Instruments X-Max 50) was used to qualitatively assess the elemental composition of 18 random particles (three particles per sample). The PM sizes analysed ranged from 2–30 μm , and large regions of agglomerated particles were present on the leaf surfaces. The Aztec Software (Oxford Instruments) was used to evaluate the chemical elements present in each sample.

3. Results and Discussion

3.1. Impact of Green Barrier on Playground Air Quality

Air quality results indicate that the green barrier has mixed impacts on Sch-GB's playground levels: a consistent decrease in NO_2 concentrations, and an environmental conditions-dependent decrease in $\text{PM}_{2.5}$ concentrations.

For NO₂, both de-seasonalised and weather-influenced data analyses indicate an overall negative concentration trend in Sheffield from 2019 to 2021 (Table 4). Not only has Sch-GB site seen a reduction in NO₂ levels since the green barrier was built in its playground, but also concentrations have decreased at both control sites. The city's NO₂ reduction is most likely related to changes in car mobility caused by COVID-19 pandemic restrictions, as the main NO₂ source in Sheffield is motorised vehicle traffic [62]. Traffic flow during post-gb21 period was most similar to pre-pandemic levels (Table 2), making it the most representative period for observing solely the green barrier's impact. Hence, comparing NO₂ concentrations from post-gb21 with pre-gb indicates that this gas pollutant decreased at all sites. However, Sch-GB had a greater reduction than City and Sch-NoGB sites (Figure S3 in Supplementary Material), suggesting that the green barrier has a mitigation effect on playground pollution levels. Subtracting Sch-GB's concentrations difference from averaged control sites' concentrations difference (Table 4), de-seasonalised results showed an NO₂ reduction of about 13% in the playground, whilst weather-influenced results showed a reduction of about 23%. It is worth noting that direct comparison of fixed monitors and diffusion tubes results is not possible due the de-seasonalisation process of the former, however, each provide complementary information about NO₂ concentration changes in time.

Table 4. De-seasonalised air pollutant mean concentrations and difference (%) against baseline scenario (pre-gb) at city scale.

Air Quality Data Collection	Period	Study Site					
		Sch-GB		City		Sch-NoGB	
		Mean ± SE (µg m ⁻³)	Conc. diff. ¹	Mean ± SE (µg m ⁻³)	Conc. diff.	Mean ± SE (µg m ⁻³)	Conc. diff.
NO ₂ —fixed monitor (de-seasonalised)	pre-gb	27.53 ± 0.05	-	19.04 ± 0.10	-	24.82 ± 0.11	-
	lock	NA ²	NA	14.37 ± 0.03	-24.43%	18.50 ± 0.03	-25.44%
	post-gb20	NA	NA	16.02 ± 0.08	-15.76%	19.02 ± 0.06	-23.34%
	post-gb21	22.88 ± 0.11	-16.88%	17.67 ± 0.10	-6.98%	24.73 ± 0.10	-0.37%
NO ₂ —diffusion tubes (weather-influenced)	pre-gb	24.58 ± 2.17	-	22.25 ± 0.66	-	28.58 ± 0.30	-
	lock	11.50 ± 1.50	-53.22%	14.22 ± 0.29	-36.09%	19.05 ± 0.31	-33.36%
	post-gb20	16.08 ± 1.17	-34.58%	17.83 ± 0.46	-19.87%	26.33 ± 0.51	-7.87%
	post-gb21	14.11 ± 0.63	-42.62%	16.43 ± 0.41	-26.16%	25.12 ± 0.59	-12.12%
PM _{2.5} —fixed monitor (de-seasonalised)	pre-gb	5.98 ± 0.01	-	6.74 ± 0.01	-	6.64 ± 0.01	-
	lock	7.50 ± 0.01	25.32%	7.96 ± 0.03	18.16%	7.98 ± 0.03	20.13%
	post-gb20	6.09 ± 0.01	1.71%	6.63 ± 0.01	-1.52%	6.62 ± 0.01	-0.27%
	post-gb21	5.85 ± 0.01	-2.31%	6.74 ± 0.01	0.033%	6.65 ± 0.01	0.078%

¹ Conc. diff. = concentration difference. ² NA = not available. Green colour indicates pollution reduction and red colour indicates pollution increase, compared to baseline period.

Furthermore, from the three study sites, only Sch-GB had a statistically significant NO₂ decrease trend over time (trend = -2.51 µg m⁻³ per year, 95% CL = -2.71, -2.19 µg m⁻³ per year, $p < 0.001$), which suggests that only the site with the GI intervention experienced a sustained NO₂ decrease from pre-gb to post-gb21 periods (Figure 6).

Spatial analysis supports the overall reduction of NO₂ in the city (Figure 7). Moreover, spatial analysis within the playground shows that for pre-gb there was a natural dilution of NO₂ from the roads, i.e., the further away from the road the diffusion tube was located, the lower the NO₂ concentration. On the other hand, once the green barrier was planted, this pattern changed. For all post GI periods, NO₂ levels were lower at diffusion tubes immediately behind the green barrier, suggesting that the greatest AQ impact covers certain range and dilutes with distance from the green barrier (Table 5 and Figure 7). Based on the [63]'s calculation of the area of protection related to green barrier's height (area of protection in metres = 3 height - 3), Sch-GB's green barrier protects up to 4.2 m behind it under ideal conditions.

In contrast to NO₂ results, de-seasonalised PM_{2.5} concentrations do not follow the same declining trend in Sheffield. PM_{2.5} levels greatly increased during the lockdown period and do not substantially differ among pre-gb, post-gb20, and post-gf-21 across the city (Table 4 and Figure S4 in Supplementary Material). Nevertheless, when comparing only pre-gb with post-gb21 as indicated above, PM_{2.5} concentrations decreased about 2% at Sch-GB's playground, whilst increasing at the control sites. Similarly to NO₂, only Sch-GB experienced a statistically significant and sustained PM_{2.5} decrease from pre-gb to post-gb21 (trend = $-0.32 \mu\text{g m}^{-3}$ per year, 95% CL = $-0.67, -0.14 \mu\text{g m}^{-3}$ per year, $p < 0.001$) (Figure 6).

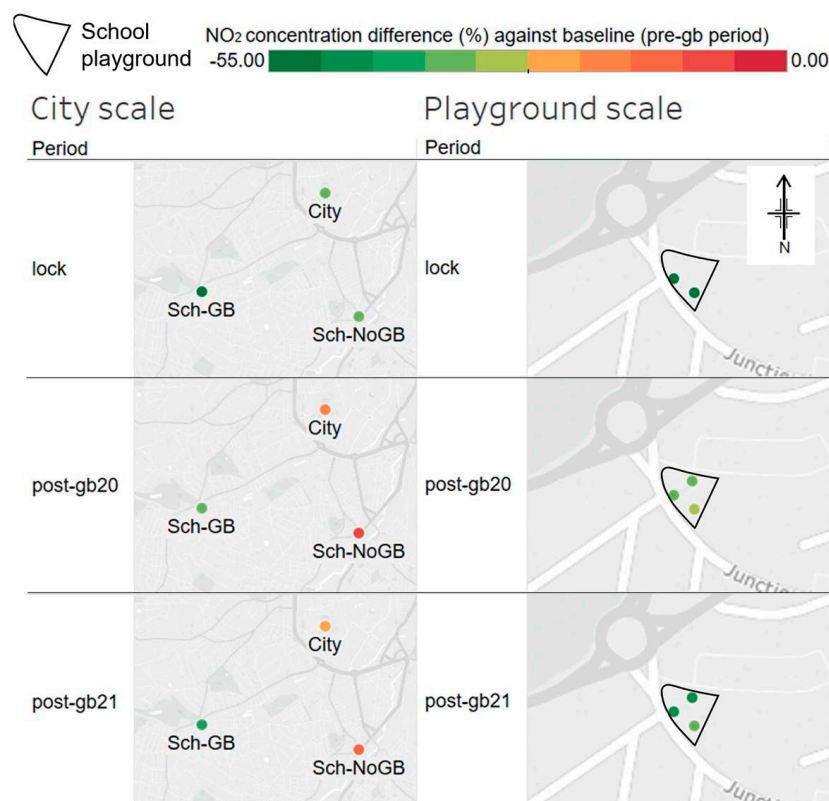


Figure 7. NO₂ mean concentrations difference (%) of sampling periods against baseline (pre-gb), data collected with diffusion tubes. Data are displayed at city scale for inter-sites comparison, and at playground scale for within site (Sch-GB) comparison.

Table 5. NO₂ mean concentrations in Sch-GB at playground scale, from diffusion tubes.

Air Quality Data Collection	Period	Location Inside Playground					
		North Tube		South Tube		West Tube	
		Mean \pm SE ($\mu\text{g m}^{-3}$)	Conc. diff. ¹	Mean \pm SE ($\mu\text{g m}^{-3}$)	Conc. diff.	Mean \pm SE ($\mu\text{g m}^{-3}$)	Conc. diff.
NO ₂ —diffusion tubes (weather-influenced)	pre-gb	24.75 \pm 2.24	-	20.75 \pm 3.33	-	28.25 \pm 2.29	-
	lock	NA	-	10.00	-51.81%	13.00	-53.98%
	post-gb20	15.75 \pm 1.11	-36.33%	14.25 \pm 1.11	-31.33%	18.25 \pm 1.11	-35.39%
	post-gb21	13.72 \pm 1.70	-44.57%	13.25 \pm 1.21	-36.14%	15.35 \pm 1.55	-45.66%

¹ Conc. diff. = concentration difference. Green colour indicates pollution reduction, compared to baseline period.

Previous studies have shown that wind direction highly influences GI's PM reduction efficiency [13,64–66]. We found that it is also the case for our PM_{2.5} de-seasonalised data at Sch-GB. Prevailing wind directions around the playground come from the west, northwest, and southeast to a lesser extent (Figure 4). Our results show that PM_{2.5} decreases with

all wind directions (PM_{2.5} trends over time are all negative and statistically significant to at least the $p < 0.05$ level, Figure 8). However, the conditional probability function visualisation at the 90th percentile (=3.5) showed that south-easterly winds bring the highest level of PM_{2.5} pollution into the playground (Figure 8). This might be related to airflow entering through the open-metal school gate (Figure 4) and could be solved by supplying the gate with a material that hinders air movement (e.g., bamboo/wooden mesh), as a GI implementation is not suitable there. Furthermore, spatial analysis signal to a more restricted airflow inside the playground due to the green barrier (Figure 9). During the pre-gb period, higher PM_{2.5} concentrations occurred on the sampling points next to the divisionary wall between the playground and the streets, and lower concentrations in the middle of the playground. Whilst for post-gb20, PM_{2.5} levels were more homogeneous across the playground.

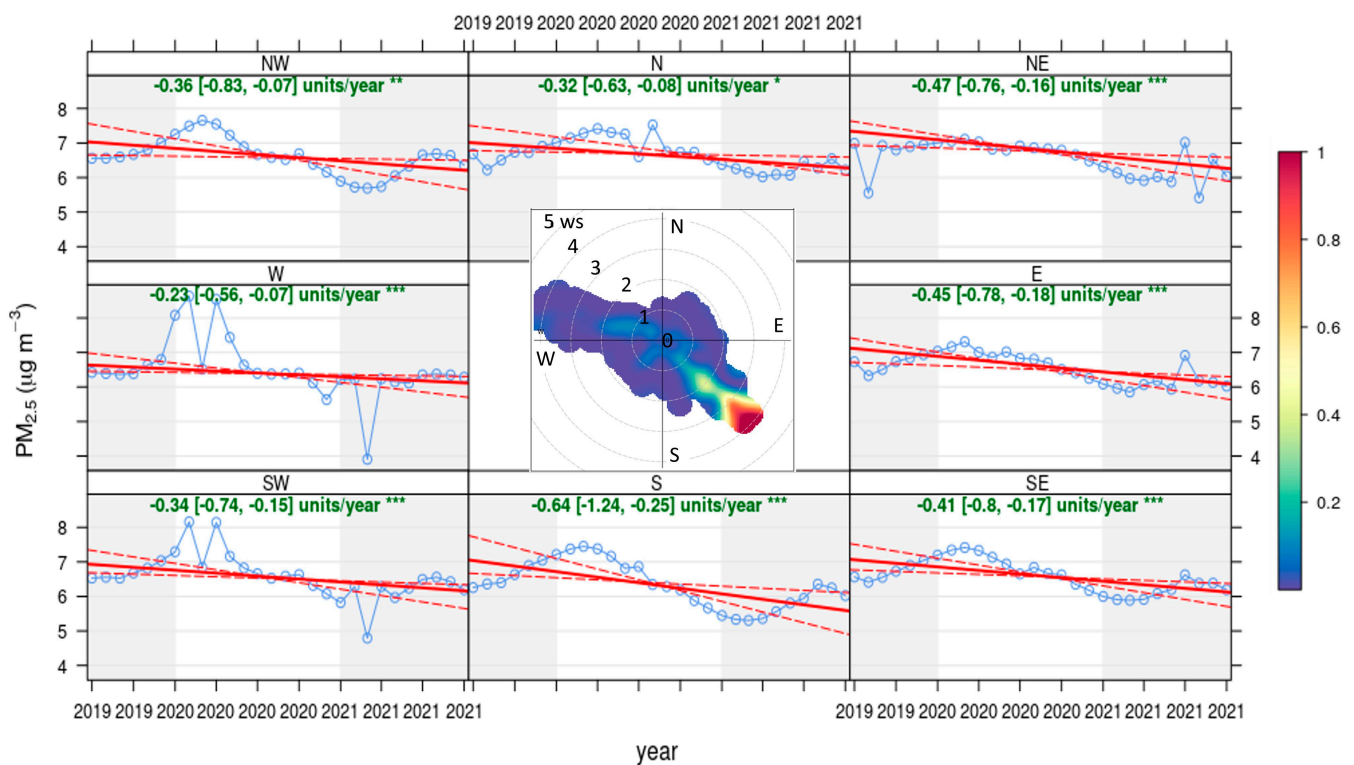


Figure 8. De-seasonalised mean PM_{2.5} concentration trends (blue line, in $\mu\text{g m}^{-3}$) by wind direction and wind speed (ws) at Sch-GB site across time. The solid red line represents the trend estimate, and the dashed red lines represent 95% confidence intervals for the trend based on resampling methods. Statistically significant trends are valid at * $p < 0.05$, ** $p < 0.01$, and *** $p < 0.001$ levels. CFP prob = conditional probability function, for the centre plot at the 90th percentile.

Other weather covariates impact PM_{2.5} concentrations, such as humidity (15.7%) and temperature (6.4%) (Figure S1), which had an influence on the data collected at children's breathing height with a mobile device. Weather-influenced results from that device showed that relatively hotter and less humid days (i.e., similar to British summer conditions) displayed a reduction in PM_{2.5} concentrations inside the playground only, in contrast to colder and more humid days (Table 6). Overall, seasonality and weather patterns have a considerable impact on PM behaviour. Despite de-seasonalised outcomes indicating a positive impact on playground air quality due to the green barrier, it is small compared to the effect of the underlying weather component.

The apparent limited protection that the green barrier provides against PM_{2.5} is possibly related to three factors: (1) the narrow width of the barrier (0.9–1.3 m), (2) the location of the fixed AQ monitor, and (3) the multiple and diverse PM sources around the playground.

Firstly, regarding GI width, research suggests that thicker green barriers are more effective at AQ provisioning [28,67,68]. Some studies suggest up to a minimum width of 10 m, although such wide thickness approach seems to be more suitable for protecting populations near long open roads, such as motorways [12]. In the urban environment, green barriers need to be more accommodating to the different landscape morphologies, where often planting space is scarce. For Sch-GB's playground, the maximum width the school could spare for planting was 1.3 m in its widest section (northwest corner), hence, plant selection assured full coverage of the green barrier's height and low porosity. As such, the green barrier in Sch-GB's playground illustrates successful multi-species GI application in an intricate urban layout, which most likely acts by deflecting air pollution. Other studies have explored the use of green barriers in open roads or urban street canyons, and conclude that GI's design should be site-specific and context-dependent to foster AQ provisioning [64,69–71]. That being said, thin green barriers (1.0–2.2 m) have a place in cities, as modelling studies have shown air pollutant reductions from 2 to 54% [66,72] and up to 42% in real life case studies [22,65,73].

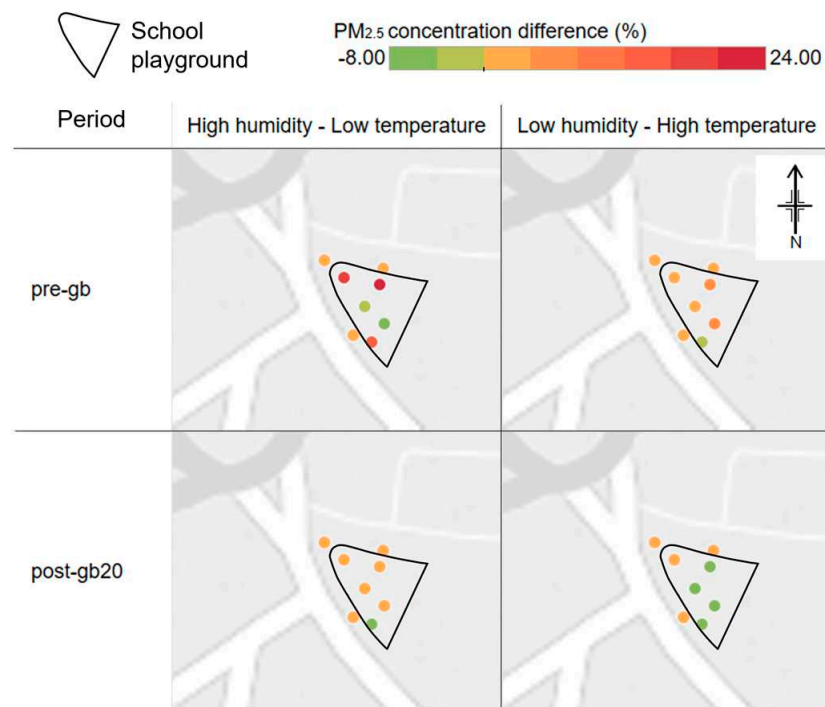


Figure 9. PM_{2.5} mean concentrations difference (%) of playground against street sampling points—data collected with mobile monitoring device. Data are displayed for two sampling periods pre-gb and post-gb20, and two weather conditions.

Secondly, the fixed AQ monitor is located on the north section of the playground, which is raised by 2 m above the ground. The monitor's installation was limited by real-life constraints of power supply access and children's safety. Its location is, therefore, higher than the sources of pollution at road level (i.e., vehicle traffic). This situation might cause the device to pick up slighter changes of air pollution because the concentrations are lower at its height. Nevertheless, evidence from PM being captured by those green barrier plants via leaf deposition is shown here (Section 3.2) and in our previous study [34], suggesting that the green barrier's PM mitigation could be more notorious had the monitor been at road level. Additionally, unlike studies where AQ was measured immediately behind the vegetation e.g., [21], our study's monitor was located 1 m away from the green barrier, which could cause a dilution effect on the pollution concentrations.

Table 6. PM_{2.5} mean concentrations and difference (%) between street and playground sampling points during two weather conditions in the Sch-GB site. Data collected with mobile monitoring device.

Weather Conditions	Period	Sampling Points	Mean ± SE (µg m ⁻³)	Conc. diff. ¹ against Street
High hum–low temp	pre-gb	street	5.82 ± 0.21	-
		playground	6.45 ± 0.20	10.95%
	post-gb20	street	7.03 ± 0.17	-
		playground	7.07 ± 0.11	0.60%
Low hum–high temp	pre-gb	street	5.63 ± 0.12	-
		playground	5.79 ± 0.11	2.79%
	post-gb20	street	6.34 ± 0.14	-
		playground	6.04 ± 0.06	-4.69%

¹ Conc. diff. = concentration difference. Green colour indicates pollution reduction and red colour indicates pollution increase, compared to mean street sampling points concentration.

Finally, sources of PM in the case study school include cars, diesel buses [56], light and heavy vehicles, and woodburning stoves from residential areas nearby. In the UK, domestic combustion accounts for 25% of the total PM_{2.5} emissions, with 70% from the use of wood as fuel [74]. Moreover, secondary PM formation caused by agriculture fertilizers used for crop growing, especially in spring, could also be a source of PM in the city. Alternatively, there might be internal sources of PM in the playground, for instance from debris plant material generated by the three mature trees on the northwest corner (Figure 4) which can be resuspended by children's movement/play. PM resuspension inside schools has been the case for sandy playgrounds in Barcelona, where sand was resuspended by children's activities and added to the local PM concentrations [75].

3.2. Elemental Composition of PM Captured by Green Barrier Plants

The green barrier plants used in the GI at Sch-GB were effective in capturing airborne PM [34], and SEM imaging revealed PM particles distributed across the leaves both individually and in regions of agglomerated particles. Figure 10 illustrates chemical analysis of a large individual pollution particle, and from an extended cluster of PM_{2.5} particles. Overall, the elemental composition of particles deposited on the green barrier plant *Hedera helix* 'Woerner', (planted along the whole length of the GI—Figure 4), indicate both natural and anthropogenic PM sources' contribution. Specifically, seventeen elements were identified on PM deposited on the *Hedera helix* leaf samples. Elements carbon (C) and oxygen (O) were found in all particles and particle clusters analysed and were the most abundant, comprising about 70–80 Wt% (mean weight percentage) and 10–20 Wt%, respectively. Iron (Fe), aluminium (Al), calcium (Ca), silicon (Si), and platinum (Pt) were the second most frequent and abundant elements. Additionally, chlorine (Cl), sulphur (S), nickel (Ni), potassium (K), phosphorus (P), sodium (Na), magnesium (Mg), Ruthenium (Ru), barium (Ba), and bromine (Br) were identified in trace levels.

The high abundance of C and O, combined with other elements identified here (P, Ca, K, Na, Fe, Cl, Mg, Al, Si) is typical of the so called 'biogenic aerosols', which are particles of biological nature (living matter, e.g., pollen, fungal spores or plant tissue) [76,77]. In addition, some of the C and O X-rays may originate from the surrounding background leaf tissue. Particles containing Si, Al, and Fe, are classified as 'geogenic particles', or natural particles derived from the Earth's crust like salts [76].

Based on the local air pollution sources, the presence of certain elements within the assessed particles is also consistent with anthropogenic origins. The significant quantity of C identified in all particle spectra partially originate from the presence of organic and elemental carbon from vehicle exhausts [78]. Moreover, C and O may also signal the presence of polycyclic aromatic hydrocarbons (PAHs), which are caused by incomplete combustion of organic matter (i.e., from diesel or petrol) and are carcinogenic [77]. Particles containing the transition metals Fe and Ni may be related to abrasion of vehicle parts, especially brake and tyre wear [79,80]. Less attention has been given to transition metals Pt

and Ru, which we found in six and two analysed regions, respectively. Pt and Ru signal traffic air pollution because they are used in motors' catalytic converters. Although the aim of catalytic converters is to transform exhaust emissions into less polluting forms, their internal catalyst rare-earth metals leak into the environment. According to Wiseman and Zereini [81], platinum group elements are increasingly found in airborne PM and, although in small concentrations, they may be more bioavailable and toxic to humans than expected. For instance, the platinum group elements are known to cause allergies, respiratory sensitisation, and oxidative damage [81,82].

EDX Spectrum with SEM Micrograph

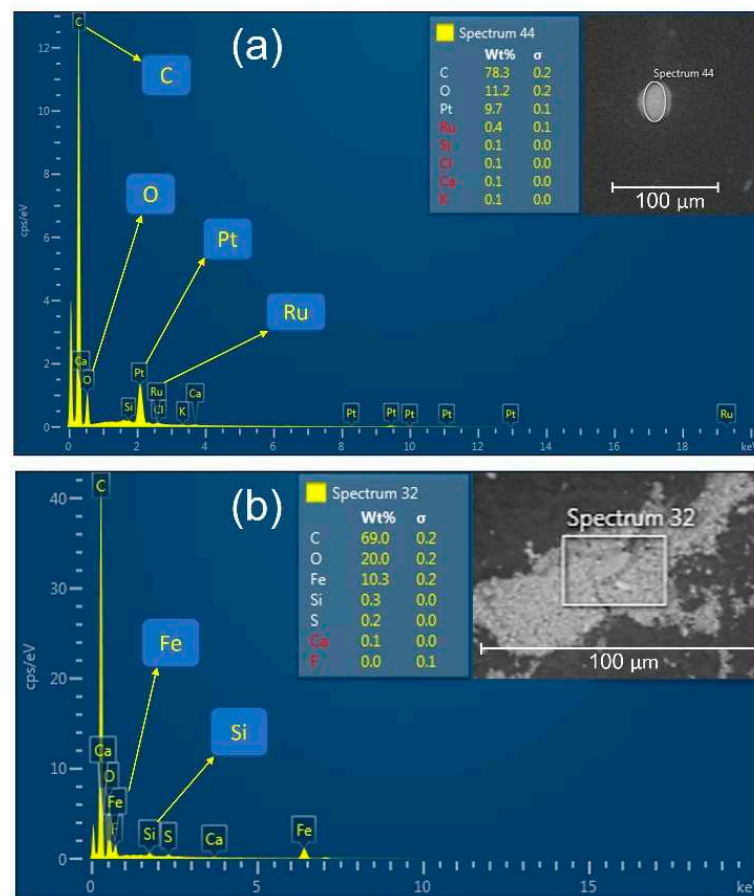


Figure 10. Sample SEM and EDX spectra of elemental composition analysis of PM captured on *Hedera helix* 'Woerner' leaves from green barrier. Each EDX spectrum shows the elements found on (a) single particle and (b) an agglomerate deposited on the leaves, and the mean weight percentage (Wt%) of each element. The SEM at the top right corner of each EDX spectrum shows PM (light grey) on the dark leaf backdrop. cps/eV = counts per second/electron Volt; σ = standard deviation.

Although it was not possible to determine the exact nature or share of each PM source in this study, the presence of Pt and Ru shows that part of the PM found here corresponds to vehicle exhaust emissions. Additionally, as leaf samples were collected in January, a winter month in the UK, vehicle traffic and home heating with solid fuels (e.g., for woodstoves) are likely to be part of the anthropogenic sources. Our results are similar to other studies that found anthropogenic elements that originate from exhaust and non-exhaust vehicle sources of PM on GI in the UK, such as living walls in Birmingham and hedges in Guildford [83,84].

Foliar PM deposition is considered a green barrier mechanism to clean the air, but secondary to air pollution dispersion effects [85]. Nevertheless, there is clear evidence on PM capture by plant structures and, therefore, a preference to include evergreen species

in green barriers [86]. Plant selection for Sch-GB's green barrier included not only five structural plants that could indeed form a barrier all year long, but species highlighted in the literature as potential PM sinks due to their micromorphological structures. SEM results here confirm PM deposition on *Hedera helix* 'Woerner' leaves, and a prior study also confirms effective PM capture by other two green barrier plants [34].

3.3. Impact of Low-Vehicle Traffic and Low-Citizens' Mobility Period (COVID-19 Lockdown) on Air Quality

Sheffield faced unexpected conditions across the two years of study due to measures imposed by the British government to control the spread of the COVID-19 disease. The global pandemic forced a strict first national lockdown from end of March to June 2020, in which people's mobility was restricted and vehicle traffic considerably decreased [31]. For the study sites, traffic flow decreased 40–64% compared to 2019 levels (Table 2). Analysis of air pollution during this exceptional lockdown period demonstrate AQ improvements regarding NO₂, but not for PM_{2.5}.

De-seasonalised data indicate that NO₂ concentrations decreased about 25% at the control sites during lockdown, which was the highest reduction of all periods (Table 4 and Figure S3 in Supplementary material). Moreover, weather-influenced results showed that Sch-GB's playground also experienced a major NO₂ reduction during lockdown, greater than post-gb20 by 18% and post-gb21 by 10% (Table 5, Figure 7). The NO₂ pollution decrease was greater at Sch-GB than at the City and Sch-NoGB sites (Table 4, Figure 7), potentially indicating a double effect of lower traffic plus green barrier. In any case, reduced traffic flow had the greatest positive impact on Sheffield's air quality regarding NO₂. This finding is consistent with vehicle traffic being the major source of NO₂ in Sheffield [62] as well as in the UK [87]. These results emphasise the importance of reducing pollution at the source as the first and most effective way to protect children's health, for example reducing motorised vehicle traffic around schools and/or preventing its proximity during pupils drop-off/pick-up times. Consequently, green infrastructure has a place in the set of measures to tackle air pollution yet, as pointed out by Hewitt et al. [88], only after 'reducing emissions and extending distance between sources and receptors'.

In contrast, PM_{2.5} levels during the lockdown period substantially increased, with an averaged de-seasonalised PM_{2.5} concentrations about 21% larger across Sheffield. Despite vehicle traffic not being the main source of PM in the city [62], a slight decrease in PM_{2.5} could have been expected from the reduced traffic's share during lockdown. However, that was not the case, and PM increased during that period as a result of other particle sources increasing. For example, domestic combustion activities increased, such as cooking or woodstove use, due to people spending more time at home. Garden fires for waste burning also saw a spike during lockdown [89], potentially adding to the local PM load. Alternatively, Munir et al. [90] attribute some of the high PM concentrations during lockdown to long-range transport of European pollution. Their study in Sheffield used back trajectory of air masses and concluded that winds originating from central and eastern Europe brought pollution and caused increases in secondary PM. Similarly to Munir et al. [90], we used the HYSPLIT model [91] to simulate PM concentrations at Sch-GB for the years 2020 and 2021 from 24–25 of April each year as an example (Figure 11). We calculated 72 h backward trajectories to assess whether 2020 and 2021 PM concentrations were under the influence of long-distance transport and source apportionment. HYSPLIT predicted higher PM concentrations arriving from Europe at those specific periods, suggesting that long-range transport of air pollution from Europe may be an important temporal source of PM at the school playground. These findings evidence the high complexity of PM formation, dispersion, and meteorology interaction. It also highlights the difficulty of PM reduction via GI or other measures.

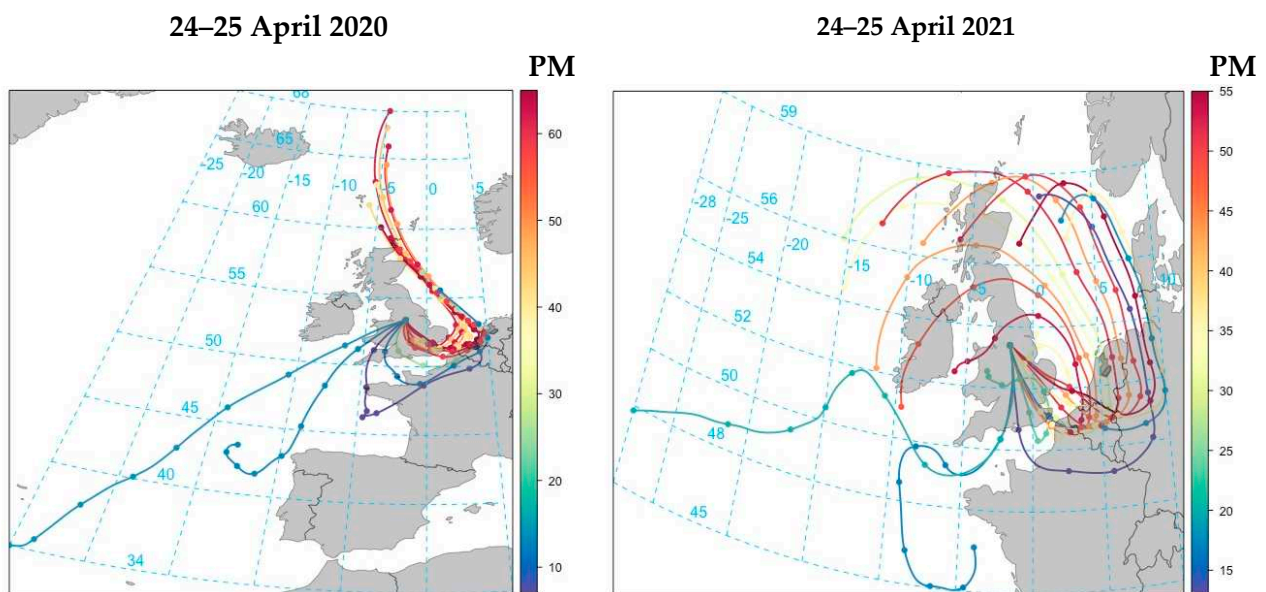


Figure 11. 72 h backward trajectories of PM concentrations ($\mu\text{g m}^{-3}$) at Sch-GB, created with the HYSPLIT model.

4. Conclusions

This study has evaluated site-specific green infrastructure, specifically multi-species thin green barriers, as an air-pollution-mitigation measure in schools. By co-creating and constructing a multi-species green barrier in a school playground with real-life design constraints, we were able to support a thriving planting scheme that mitigates air pollution to real levels. The methods selected for this research allowed us to answer our three research questions (Section 1):

- i. This study suggests that the site-specific and multi-species thin green barrier (0.9–1.3 m max width) built in a UK school playground reduced air pollution. The reduction in pollutants concentration was significant for NO_2 (between 13% to 23%) and slight for $\text{PM}_{2.5}$ (about 2%). The downward pre-post intervention trend was statistically significant.
- ii. Composition of PM deposited on the green barrier plant *Hedera helix* ‘Woerner’ suggests PM of natural and anthropogenic origin. The latter include catalytic converters from motorised vehicles.
- iii. Low-vehicle traffic and low-citizen mobility (lockdown) seem to have significantly reduced NO_2 ; such reduction exceeds the effects of the green barrier. These mobility restrictions do not seem to significantly reduce PM pollution in the UK case study, most likely because meteorological patterns and conditions have a stronger influence on PM than traffic levels.

The mitigation effect of the multi-species thin green barrier on school AQ—most likely due to air pollutant deflection/dispersion by the green barrier, yet PM deposition was also identified—was quantifiable, and potentially helped to further reduce air pollution in the school playground during the first COVID-19 lockdown (which imposed travel restrictions). The reduced traffic flow during lockdown, however, caused the greatest reduction of NO_2 in Sheffield (about 25% at the control sites). This finding highlights the importance of working towards systematic changes, such as cars’ phasing out, low traffic neighbourhoods, and school streets initiatives, to make a direct and strong impact on air pollution mitigation and protect children’s health. $\text{PM}_{2.5}$ did not decrease during the lockdown period, rather, it increased. This behaviour was caused by an array of potential sources including increased domestic burning (e.g., cooking and heating) during lockdown, spring fertilizer pollution, continued diesel bus services, and long-range transport of air pollution from central and

eastern Europe. The variety of PM sources highlights the volatility and difficulty of PM pollution mitigation due to its interrelation with meteorology and its cross-continental range, making a case for site-specific intervention to improve local air quality, such as green barriers in school playgrounds.

This study was constrained by the nature of the school's built-up environment, the reduced green barrier width to maintain play space, and by the plant selection which was localised to the UK climate. In addition, air quality is a topic of concern in the UK compared to other geographies [92], and actions to minimise pollution could be taken by its citizens (i.e., active travel). Therefore, further studies looking at real-case scenario green barriers with different plant mixes and in other climates or geographies could help to supplement our findings and the green barrier design.

Green barriers can improve school air quality, and, despite their limited potential, changes are quantifiable and significant even in our space-constrained site. Moreover, this nature-based solution can complement other tools and efforts to create healthy environments for children, as well as offer multiple co-benefits to the school community due to the added greenery.

Supplementary Materials: The following supporting information can be downloaded at: <https://www.mdpi.com/article/10.3390/su15021075/s1>, Figure S1: Model results and partial dependency of the covariates on PM_{2.5} and NO₂ concentrations at Sch-GB from 2019 to 2021; Figure S2: Taylor diagram comparing the modelled data (red dot) which are the corrected low-cost mobile device measurements for the reference data (observed); Figure S3: De-seasonalised NO₂ concentrations ($\mu\text{g m}^{-3}$) for each data-collection period and study site; and Figure S4: De-seasonalised PM_{2.5} concentrations ($\mu\text{g m}^{-3}$) for each data-collection period and study site.

Author Contributions: Conceptualisation, M.d.C.R.B., M.V.M. and R.W.C.; Methodology, M.d.C.R.B., R.C., M.V.M. and B.J.I.; Data curation and formal analysis, R.C. (fixed monitors data), M.d.C.R.B. (mobile monitor, diffusion tubes data and SEM/EDX); Writing—original draft preparation, M.d.C.R.B. and R.C.; Writing—review and editing, M.d.C.R.B., R.C., M.V.M. and B.J.I.; Project administration, M.d.C.R.B.; Supervision, M.V.M., R.W.C. and B.J.I.; Funding acquisition, M.V.M., R.W.C. and B.J.I. All authors have read and agreed to the published version of the manuscript.

Funding: M.d.C.R.B. and R.C. acknowledge the funding from the Grantham Centre for Sustainable Futures, The University of Sheffield for PhD studentships. M.V.M. acknowledges funding from the UKRI Future Leaders Fellowship Programme (MR/T019867/1).

Institutional Review Board Statement: Not applicable.

Informed Consent Statement: Not applicable.

Data Availability Statement: The data generated here are accessible at <https://doi.org/10.15131/shef.data.21559671>. For the purpose of open access, the author has applied a Creative Commons Attribution (CC BY) licence to any Author Accepted Manuscript version arising.

Acknowledgments: We thank the case study school for providing space and time to make this research project a reality. Additional thanks to Urban Wilderness for providing the planting plans modified here. We acknowledge the Electron Microscopy Service, Department of Molecular Biology and Biotechnology at the University of Sheffield for their support with SEM/EDX analysis.

Conflicts of Interest: The authors declare no conflict of interest.

References

1. WHO. *Air Pollution and Child Health: Prescribing Clean Air Summary*; WHO: Geneva, Switzerland, 2018.
2. Calderón-Garcidueñas, L.; Engle, R.; Mora-Tiscareño, A.; Styner, M.; Gómez-Garza, G.; Zhu, H.; Jewells, V.; Torres-Jardón, R.; Romero, L.; Monroy-Acosta, M.E.; et al. Exposure to severe urban air pollution influences cognitive outcomes, brain volume and systemic inflammation in clinically healthy children. *Brain Cogn.* **2011**, *77*, 345–355. [[CrossRef](#)] [[PubMed](#)]
3. Freire, C.; Ramos, R.; Puertas, R.; Lopez Espinosa, M.J.; Julvez, J.; Aguilera, I.; Cruz, F.; Fernandez, M.F.; Sunyer, J.; Olea, N. Association of traffic-related air pollution with cognitive development in children. *J. Epidemiol. Community Health* **2010**, *64*, 223–228. [[CrossRef](#)]

4. Roberts, S.; Arseneault, L.; Barratt, B.; Beevers, S.; Danese, A.; Odgers, C.L.; Moffitt, T.E.; Reuben, A.; Kelly, F.J.; Fisher, H.L. Exploration of NO₂ and PM_{2.5} air pollution and mental health problems using high-resolution data in London-based children from a UK longitudinal cohort study. *Psychiatry Res.* **2019**, *272*, 8–17. [CrossRef] [PubMed]
5. An, F.; Liu, J.; Lu, W.; Jareemit, D. A review of the effect of traffic-related air pollution around schools on student health and its mitigation. *J. Transp. Health* **2021**, *23*, 101249. [CrossRef]
6. Brugha, R.; Grigg, J. Urban air pollution and respiratory infections. *Paediatr. Respir. Rev.* **2014**, *15*, 194–199. [CrossRef]
7. Payne-Sturges, D.C.; Marty, M.A.; Perera, F.; Miller, M.D.; Swanson, M.; Ellickson, K.; Cory-Slechta, D.A.; Ritz, B.; Balmes, J.; Anderko, L.; et al. Healthy air, healthy brains: Advancing air pollution policy to protect children’s health. *Am. J. Public Health* **2019**, *109*, 550–554. [CrossRef]
8. Sofia, D.; Gioiella, F.; Lotrecchiano, N.; Giuliano, A. Mitigation strategies for reducing air pollution. *Environ. Sci. Pollut. Res.* **2020**, *27*, 19226–19235. [CrossRef] [PubMed]
9. Amann, M.; Kieseewetter, G.; Schöpp, W.; Klimont, Z.; Winiwarter, W.; Cofala, J.; Rafaj, P.; Höglund-Isaksson, L.; Gomez-Sabriana, A.; Heyes, C.; et al. Reducing global air pollution: The scope for further policy interventions: Achieving clean air worldwide. *Philos. Trans. R. Soc. A* **2020**, *378*, 2183. [CrossRef]
10. European Commission. *Green Infrastructure (GI)—Enhancing Europe’s Natural Capital*; European Commission: Brussels, Belgium, 2013.
11. del Bermúdez, M.C.R. Plants, Ambient Air Quality, and Human Health. In *Good Health and Well-Being. Encyclopedia of the UN Sustainable Development Goals*; Leal Filho, W., Wall, T., Azul, A.M., Brandli, L., Özuyar, P.G., Eds.; Springer: Cham, Switzerland, 2020; pp. 1–12. ISBN 9783319696270.
12. Baldauf, R. Air pollution mitigation through vegetation barriers and green space. In *Traffic-Related Air Pollution*; Elsevier Inc.: Amsterdam, The Netherlands, 2020; pp. 437–453. ISBN 9780128181225.
13. Deshmukh, P.; Isakov, V.; Venkatram, A.; Yang, B.; Zhang, K.M.; Logan, R.; Baldauf, R. The effects of roadside vegetation characteristics on local, near-road air quality. *Air Qual. Atmos. Health* **2019**, *12*, 259–270. [CrossRef]
14. Grote, R.; Samson, R.; Alonso, R.; Amorim, J.H.; Cariñanos, P.; Churkina, G.; Fares, S.; Thiec, D.L.; Niinemets, Ü.; Mikkelsen, T.N.; et al. Functional traits of urban trees: Air pollution mitigation potential. *Front. Ecol. Environ.* **2016**, *14*, 543–550. [CrossRef]
15. US EPA. *Best Practices for Reducing Near-Road Pollution Exposure at Schools*; US EPA: Washington, DC, USA, 2015.
16. Landscape & Urban Design. Highlighting Britain’s toxic air scandal: How C4’s dispatches & Hedges Direct reduced air pollution by 53%. *Landsc. Urban Des.* **2019**, *38*, 58–59. Available online: <https://viewer.joomag.com/landscape-urban-design-issue-38-2019/0706808001561646708?short&> (accessed on 20 July 2022).
17. Groundwork. *Air Quality Green Infrastructure: A Toolkit for Schools*; Groundwork: London, UK, 2019.
18. BBC. *Newsround Air pollution: How a School in Manchester Is Fighting Back against Air Pollution*; BBC: London, UK, 2021.
19. Barrett, T. ‘Life-Saving’ Scheme to Tackle Air Pollution at Manchester Schools. 2019. Available online: <https://airqualitynews.com/2019/06/24/life-saving-scheme-to-tackle-air-pollution-at-manchester-schools/> (accessed on 4 April 2022).
20. Mayor of London Press Office. *Mayor’s Green Fund Helps Schools Fight Toxic Air*; Mayor of London Press Office: London, UK, 2019.
21. Abhijith, K.V.; Kukadia, V.; Kumar, P. Investigation of air pollution mitigation measures, ventilation, and indoor air quality at three schools in London. *Atmos. Environ.* **2022**, *289*, 119303. [CrossRef]
22. Al-dabbous, A.N.; Kumar, P. The influence of roadside vegetation barriers on airborne nanoparticles and pedestrians exposure under varying wind conditions. *Atmos. Environ.* **2014**, *90*, 113–124. [CrossRef]
23. Chang, W.R. Effect of porous hedge on cross ventilation of a residential building. *Build. Environ.* **2006**, *41*, 549–556. [CrossRef]
24. Xing, Y.; Brimblecombe, P. Role of vegetation in deposition and dispersion of air pollution in urban parks. *Atmos. Environ.* **2019**, *201*, 73–83. [CrossRef]
25. Jayasooriya, V.M.; Ng, A.W.M.; Muthukumar, S.; Perera, B.J.C. Green infrastructure practices for improvement of urban air quality. *Urban For. Urban Green.* **2017**, *21*, 34–47. [CrossRef]
26. Jeanjean, A.P.R.; Gallagher, J.; Monks, P.S.; Leigh, R.J. Ranking current and prospective NO₂ pollution mitigation strategies: An environmental and economic modelling investigation in Oxford Street, London. *Environ. Pollut.* **2017**, *225*, 587–597. [CrossRef]
27. Pugh, T.A.M.; MacKenzie, A.R.; Whyatt, J.D.; Hewitt, C.N. Effectiveness of green infrastructure for improvement of air quality in urban street canyons. *Environ. Sci. Technol.* **2012**, *46*, 7692–7699. [CrossRef]
28. Morakinyo, T.E.; Lam, Y.F. Simulation study of dispersion and removal of particulate matter from traffic by road-side vegetation barrier. *Environ. Sci. Pollut. Res.* **2016**, *23*, 6709–6722. [CrossRef]
29. Maher, B.A.; Gonet, T.; Karloukovski, V.V.; Wang, H.; Bannan, T.J. Protecting playgrounds: Local-Scale reduction of airborne particulate matter concentrations through particulate deposition on roadside ‘tredges’ (green infrastructure). *Sci. Rep.* **2022**, *12*, 14236. [CrossRef] [PubMed]
30. UK Department for Transport Road Traffic Statistics—Local Authority Sheffield. Available online: <https://roadtraffic.dft.gov.uk/local-authorities/159> (accessed on 20 July 2022).
31. Institute for Government Timeline of UK Government Coronavirus Lockdowns and Restrictions. Available online: <https://www.instituteforgovernment.org.uk/charts/uk-government-coronavirus-lockdowns> (accessed on 4 April 2022).
32. Ortiz, P.F. Urban Flows Observatory Portal. Available online: <https://sheffield-portal.urbanflows.ac.uk/ufobin/ufportal/> (accessed on 30 October 2021).

33. Redondo-Bermúdez, M.d.C.; Jorgensen, A.; Cameron, R.W.; Val Martin, M. Green Infrastructure for Air Quality plus (GI4AQ+): Defining critical dimensions for implementation in schools and the meaning of ‘plus’ in a UK context. *Nat.-Based Solut.* **2022**, *2*, 2–13. [CrossRef]
34. Redondo-Bermúdez, M.d.C.; Gulenc, I.T.; Cameron, R.W.; Inkson, B.J. ‘Green barriers’ for air pollutant capture: Leaf micromorphology as a mechanism to explain plants capacity to capture particulate matter. *Environ. Pollut.* **2021**, *288*, 117809. [CrossRef] [PubMed]
35. Chakraborty, R.; Heydon, J.; Mayfield, M.; Mihaylova, L. Indoor air pollution from residential stoves: Examining the flooding of particulate matter into homes during real-world use. *Atmosphere* **2020**, *11*, 1326. [CrossRef]
36. Munir, S.; Mayfield, M.; Coca, D.; Jubb, S.A. Structuring an integrated air quality monitoring network in large urban areas—Discussing the purpose, criteria and deployment strategy. *Atmos. Environ. X* **2019**, *2*, 100027. [CrossRef]
37. Environmental Instruments Ltd Global Co-Location Comparison Trials. Available online: <https://www.aqmesh.com/performance/co-location-comparison-trials/> (accessed on 20 May 2022).
38. Breathe London. *Breathe London Technical Report. Pilot Phase (2018–2020)*; Breathe London: London, UK, 2021.
39. Zauli-Sajani, S.; Marchesi, S.; Pironi, C.; Barbieri, C.; Poluzzi, V.; Colacci, A. Assessment of air quality sensor system performance after relocation. *Atmos. Pollut. Res.* **2021**, *12*, 282–291. [CrossRef]
40. Merico, E.; Dinoi, A.; Contini, D. Development of an integrated modelling-measurement system for near-real-time estimates of harbour activity impact to atmospheric pollution in coastal cities. *Transp. Res. Part D* **2019**, *73*, 108–119. [CrossRef]
41. Wong, P.P.Y.; Lai, P.C.; Allen, R.; Cheng, W.; Lee, M.; Tsui, A.; Tang, R.; Thach, T.Q.; Tian, L.; Brauer, M.; et al. Vertical monitoring of traffic-related air pollution (TRAP) in urban street canyons of Hong Kong. *Sci. Total Environ.* **2019**, *670*, 696–703. [CrossRef]
42. Mohammed, W.; Shantz, N.; Neil, L.; Townend, T.; Adamescu, A.; Al-Abadleh, H.A. Air Quality Measurements in Kitchener, Ontario, Canada Using Multisensor Mini Monitoring Stations. *Atmosphere* **2022**, *13*, 83. [CrossRef]
43. Castell, N.; Schneider, P.; Grossberndt, S.; Fredriksen, M.F.; Sousa-Santos, G.; Vogt, M.; Bartonova, A. Localized real-time information on outdoor air quality at kindergartens in Oslo, Norway using low-cost sensor nodes. *Environ. Res.* **2018**, *165*, 410–419. [CrossRef]
44. Environmental Instruments Ltd. AQ Mesh an Air Quality Monitoring System. Available online: <https://www.aqmesh.com/products/aqmesh/> (accessed on 18 November 2021).
45. UK Air Information Resource Site Information for Sheffield Devonshire Green (UKA00575). Available online: https://uk-air.defra.gov.uk/networks/site-info?uka_id=UKA00575 (accessed on 19 November 2021).
46. Sheffield City Council Air quality in Sheffield. Available online: <https://www.sheffield.gov.uk/home/pollution-nuisance/air-quality> (accessed on 19 November 2021).
47. DEFRA Diffusion Tubes Overview. Available online: <https://laqm.defra.gov.uk/air-quality/air-quality-assessment/diffusion-tubes-overview/> (accessed on 10 March 2022).
48. Loader, A. *NO2 Diffusion Tubes for LAQM: Guidance Note for Local Authorities*; DEFRA: Didcot, UK, 2006.
49. Sheffield City Council Map of Diffusion Tubes. Available online: <https://sheffieldcc.maps.arcgis.com/apps/webappviewer/index.html?id=199b788e3efc4bfdb75be866cf3bd01e> (accessed on 2 February 2022).
50. Oguntoko, O.; Emoruwa, F.O.; Taiwo, M.A. Assessment of air pollution and health hazard associated with sawmill and municipal waste burning in Abeokuta Metropolis, Nigeria. *Environ. Sci. Pollut. Res.* **2019**, *26*, 32708–32722. [CrossRef] [PubMed]
51. Embiale, A.; Zewge, F.; Chandravanshi, B.S.; Sahle-Demessie, E. Commuter exposure to particulate matters and total volatile organic compounds at roadsides in Addis Ababa, Ethiopia. *Int. J. Environ. Sci. Technol.* **2019**, *16*, 4761–4774. [CrossRef]
52. Apparicio, P.; Gelb, J.; Carrier, M.; Mathieu, M.È.; Kingham, S. Exposure to noise and air pollution by mode of transportation during rush hours in Montreal. *J. Transp. Geogr.* **2018**, *70*, 182–192. [CrossRef]
53. Urban Flows Observatory The MOBIUS Project. Available online: <https://urbanflows.ac.uk/mobius/> (accessed on 18 November 2021).
54. Bao, R.; Zhang, A. Does lockdown reduce air pollution? Evidence from 44 cities in northern China. *Sci. Total Environ.* **2020**, *731*, 139052. [CrossRef]
55. Menut, L.; Bessagnet, B.; Siour, G.; Mailler, S.; Pennel, R.; Cholakian, A. Impact of lockdown measures to combat COVID-19 on air quality over western Europe. *Sci. Total Environ.* **2020**, *741*, 140426. [CrossRef]
56. Ropkins, K.; Tate, J.E. Early observations on the impact of the COVID-19 lockdown on air quality trends across the UK. *Sci. Total Environ.* **2021**, *754*, 142374. [CrossRef]
57. Mohajeri, N.; Walch, A.; Gudmundsson, A.; Heaviside, C.; Askari, S.; Wilkinson, P.; Davies, M. COVID-19 mobility restrictions: Impacts on urban air quality and health. *BUILD. Cities* **2021**, *2*, 759–788. [CrossRef]
58. Carslaw, D.C. Deweather—An R Package to Remove Meteorological Variation from Air Quality Data. Available online: <https://github.com/davidcarslaw/deweather> (accessed on 10 December 2021).
59. Ridgeway, G. gbm—Generalized Boosted Models. R Package. Available online: <https://cran.r-project.org/package=gbm> (accessed on 3 January 2022).
60. Carslaw, D.C. Worldmet—R Package for Accessing NOAA Integrated Surface Database (ISD) Meteorological Observations. Available online: <https://davidcarslaw.github.io/worldmet/> (accessed on 3 January 2022).
61. Carslaw, D.C.; Ropkins, K. Openair—An R package for air quality data analysis. *Environ. Model. Softw.* **2012**, *27–28*, 52–61. [CrossRef]

62. Munir, S.; Mayfield, M.; Coca, D.; Mihaylova, L.S.; Osammor, O. Analysis of air pollution in urban areas with airviro dispersion model—A case study in the city of Sheffield, United Kingdom. *Atmosphere* **2020**, *11*, 285. [CrossRef]
63. Greater London Authority. *Using Green Infrastructure to Protect People from Air Pollution*; Greater London Authority: London, UK, 2019.
64. Abhijith, K.V.; Kumar, P.; Gallagher, J.; Mcnabola, A.; Baldauf, R.; Pilla, F.; Broderick, B.; Di Sabatino, S.; Pulvirenti, B. Air pollution abatement performances of green infrastructure in open road and built-up street canyon environments—A review. *Atmos. Environ.* **2017**, *162*, 71–86. [CrossRef]
65. Kumar, P.; Zavala-Reyes, J.C.; Tomson, M.; Kalaiarasan, G. Understanding the effects of roadside hedges on the horizontal and vertical distributions of air pollutants in street canyons. *Environ. Int.* **2022**, *158*, 106883. [CrossRef]
66. Pearce, H.; Levine, J.G.; Cai, X.; MacKenzie, A.R. Introducing the Green Infrastructure for Roadside Air Quality (GI4RAQ) Platform: Estimating Site-Specific Changes in the Dispersion of Vehicular Pollution Close to Source. *Forests* **2021**, *12*, 769. [CrossRef]
67. Baldauf, R. Roadside vegetation design characteristics that can improve local, near-road air quality. *Transp. Res. Part D* **2017**, *52*, 354–361. [CrossRef] [PubMed]
68. Neft, I.; Scungio, M.; Culver, N.; Singh, S. Simulations of aerosol filtration by vegetation: Validation of existing models with available lab data and application to near-roadway scenario. *Aerosol. Sci. Technol.* **2016**, *50*, 937–946. [CrossRef]
69. Morakinyo, T.E.; Lam, Y.F.; Hao, S. Evaluating the role of green infrastructures on near-road pollutant dispersion and removal: Modelling and measurement. *J. Environ. Manag.* **2016**, *182*, 595–605. [CrossRef] [PubMed]
70. Tiwari, A.; Kumar, P.; Baldauf, R.; Zhang, K.M.; Pilla, F.; Di Sabatino, S.; Brattich, E.; Pulvirenti, B. Considerations for evaluating green infrastructure impacts in microscale and macroscale air pollution dispersion models. *Sci. Total Environ.* **2019**, *672*, 410–426. [CrossRef]
71. Tomson, M.; Kumar, P.; Barwise, Y.; Perez, P.; Forehead, H.; French, K.; Morawska, L.; Watts, J.F. Green infrastructure for air quality improvement in street canyons. *Environ. Int.* **2021**, *146*, 106288. [CrossRef]
72. Li, X.B.; Lu, Q.C.; Lu, S.J.; He, H.D.; Peng, Z.R.; Gao, Y.; Wang, Z.Y. The impacts of roadside vegetation barriers on the dispersion of gaseous traffic pollution in urban street canyons. *Urban For. Urban Green.* **2016**, *17*, 80–91. [CrossRef]
73. Temper, A.H.; Green, D.C. *The Impact of a Green Screen on Concentrations of Nitrogen Dioxide at Bowes Primary School, Enfield*; Prepared for the London Borough of Enfield; King's College London: London, UK, 2018; pp. 1–19.
74. DEFRA Emissions of Air Pollutants in the UK—Particulate Matter (PM10 and PM2.5). Available online: <https://www.gov.uk/government/statistics/emissions-of-air-pollutants/emissions-of-air-pollutants-in-the-uk-particulate-matter-pm10-and-pm25#major-emission-sources-for-pm10-and-pm25-in-the-uk> (accessed on 10 April 2022).
75. Amato, F.; Rivas, I.; Viana, M.; Moreno, T.; Bouso, L.; Reche, C.; Álvarez-Pedrerol, M.; Alastuey, A.; Sunyer, J.; Querol, X. Sources of indoor and outdoor PM_{2.5} concentrations in primary schools. *Sci. Total Environ.* **2014**, *490*, 757–765. [CrossRef]
76. Zeb, B.; Alam, K.; Sorooshian, A.; Blaschke, T.; Ahmad, I.; Shahid, I. On the morphology and composition of particulate matter in an urban environment. *Aerosol. Air Qual. Res.* **2018**, *18*, 1431–1447. [CrossRef]
77. Pachauri, T.; Singla, V.; Satsangi, A.; Lakhani, A.; Maharaj Kumari, K. SEM-EDX characterization of individual coarse particles in Agra, India. *Aerosol. Air Qual. Res.* **2013**, *13*, 523–536. [CrossRef]
78. Zhang, Z.H.; Khlystov, A.; Norford, L.K.; Tan, Z.K.; Balasubramanian, R. Characterization of traffic-related ambient fine particulate matter (PM_{2.5}) in an Asian city: Environmental and health implications. *Atmos. Environ.* **2017**, *161*, 132–143. [CrossRef]
79. Pant, P.; Harrison, R.M. Estimation of the contribution of road traffic emissions to particulate matter concentrations from field measurements: A review. *Atmos. Environ.* **2013**, *77*, 78–97. [CrossRef]
80. Gonet, T.; Maher, B.A.; Kukutschová, J. Source apportionment of magnetite particles in roadside airborne particulate matter. *Sci. Total Environ.* **2021**, *752*, 141828. [CrossRef] [PubMed]
81. Wiseman, C.L.S.; Zereini, F. Airborne particulate matter, platinum group elements and human health: A review of recent evidence. *Sci. Total Environ.* **2009**, *407*, 2493–2500. [CrossRef]
82. Ravindra, K.; Bencs, L.; Van Grieken, R. Platinum group elements in the environment and their health risk. *Sci. Total Environ.* **2004**, *318*, 1–43. [CrossRef]
83. Weerakkody, U.; Dover, J.W.; Mitchell, P.; Reiling, K. Particulate matter pollution capture by leaves of seventeen living wall species with special reference to rail-traffic at a metropolitan station. *Urban For. Urban Green.* **2017**, *27*, 173–186. [CrossRef]
84. Abhijith, K.V.; Kumar, P. Quantifying particulate matter reduction and their deposition on the leaves of green infrastructure. *Environ. Pollut.* **2020**, *265*, 114884. [CrossRef]
85. Diener, A.; Mudu, P. How can vegetation protect us from air pollution? A critical review on green spaces' mitigation abilities for air-borne particles from a public health perspective—With implications for urban planning. *Sci. Total Environ.* **2021**, *796*, 148605. [CrossRef]
86. Barwise, Y.; Kumar, P. Designing vegetation barriers for urban air pollution abatement: A practical review for appropriate plant species selection. *Clim. Atmos. Sci.* **2020**, *3*, 12. [CrossRef]
87. DEFRA Emissions of Air Pollutants in the UK—Nitrogen Oxides (NOx). Available online: <https://www.gov.uk/government/statistics/emissions-of-air-pollutants/emissions-of-air-pollutants-in-the-uk-nitrogen-oxides-nox> (accessed on 17 May 2022).
88. Hewitt, C.N.; Ashworth, K.; Mackenzie, A.R. Using green infrastructure to improve urban air quality (GI4AQ). *Ambio* **2019**, *49*, 62–73. [CrossRef]

89. London Fire Brigade. *London Lockdown Sees Spike in Outdoor Fires*; London Fire Brigade: London, UK, 2020.
90. Munir, S.; Coskuner, G.; Jassim, M.S.; Aina, Y.A.; Ali, A.; Mayfield, M. Changes in air quality associated with mobility trends and meteorological conditions during COVID-19 lockdown in Northern England, UK. *Atmosphere* **2021**, *12*, 504. [[CrossRef](#)]
91. Stein, A.F.; Draxler, R.R.; Rolph, G.D.; Stunder, B.J.B.; Cohen, M.D.; Ngan, F. NOAA's HYSPLIT Atmospheric Transport and Dispersion Modeling System. *Bull. Am. Meteorol. Soc.* **2015**, *96*, 2059–2077. [[CrossRef](#)]
92. Redondo Bermúdez, M. del C.; Kanai, J.M.; Astbury, J.; Fabio, V.; Jorgensen, A. Green Fences for Buenos Aires: Implementing Green Infrastructure for (More than) Air Quality. *Sustainability* **2022**, *14*, 4129. [[CrossRef](#)]

Disclaimer/Publisher's Note: The statements, opinions and data contained in all publications are solely those of the individual author(s) and contributor(s) and not of MDPI and/or the editor(s). MDPI and/or the editor(s) disclaim responsibility for any injury to people or property resulting from any ideas, methods, instructions or products referred to in the content.